

## Parametric Lower-Hybrid Instability Driven by Modulated Electron-Beam Injection

G. R. Allen, D. K. Owens, S. W. Seiler, and M. Yamada  
*Plasma Physics Laboratory, Princeton University, Princeton, New Jersey 08540*

and

H. Ikezi  
*Bell Laboratories, Murray Hill, New Jersey 07974*

and

M. Porkolab  
*Department of Physics and Plasma Fusion Center, Massachusetts Institute of Technology, Cambridge, Massachusetts 02139*

(Received 17 July 1978)

A modulated electron beam is injected into a low- $\beta$  plasma parallel to the confining field to investigate the energy-transfer rate from the electron beam to the plasma. Parametric excitation of electrostatic lower-hybrid waves and ion-cyclotron quasimodes is experimentally identified. The temperature of both ions and electrons is observed to increase significantly concomitant with the growth of the instability.

Plasma heating by high-energy particle-beam injection is considered to be one of the most promising methods of obtaining the ion temperatures necessary for a thermonuclear plasma. Relativistic-electron-beam injection has the advantages of high-energy density, easy beam production, and efficient beam-target energy transfer.<sup>1</sup> The mechanism by which the beam transfers its energy to the target plasma has been a subject of intensive research.<sup>1-5</sup>

In the present experiment an electron beam injected parallel to the confining magnetic field ( $B = 2-6$  kG) of a low- $\beta$ , isothermal ( $T_e \approx T_i$ ) plasma is density modulated at or above the lower-hybrid frequency ( $\omega_{LH}$ ) of the target plasma. We observe that such a modulation can parametrically excite a lower-hybrid wave and either an ion quasimode or an ion-cyclotron mode.<sup>8-11</sup> The significant contributions of this work are the detailed measurements of the subsequent parametric instability, including the frequency and wave-number matching of the decay process ( $\omega_0 = \omega_1 + \omega_2$ ,  $\vec{k}_0 = \vec{k}_1 + \vec{k}_2$ ), the dispersion relations, and the electron- and time-dependent ion heating caused by the instability. The observed anomalous beam-plasma energy-transfer rate ( $T_{i0}^{-1} dT_i/dt \sim 100 \mu\text{sec}$ ) is  $\sim 10^4$  times faster than classical collisional energy transfer.

The experiments were performed in the thermally ionized potassium plasma of the Princeton Q-1 device converted into a double-plasma machine, as shown in Fig. 1.<sup>5,12</sup> A negatively biased mesh divides the plasma column (3.2 cm diam)

into a beam-extraction plasma and an 87-cm long ( $\cong L$ ) target plasma ( $n_e \approx 10^9 \text{ cm}^{-3}$ ,  $T_e \approx 0.3$  eV,  $T_i \approx 0.4$  eV; probes show that all radial profiles are flat out to  $r = 16$  mm). With the target ionizer plate grounded and the beam-ionizer plate biased ( $V_b \sim -12$  V) such that the potential of the driving plasma is 2-3 V less negative than  $V_{\text{mesh}}$ , a suprathermal electron beam (current  $\sim 1$  mA) is driven into the target plasma. The beam is defined by a mechanical aperture (6 mm diam) and has a velocity  $v_b \approx (-2eV_{\text{bias}}/m_e)^{1/2}$  and density

$$n_b \propto n_e (-eV_{\text{bias}}/T_e)^{1/2} \exp[e\Delta V_{\text{mesh}}/T_e].$$

The sharp radial drop in plasma potential at the edge of the electron beam results in a strong radial electric field, and with an unmodulated high-density beam, the cross-field electron current ( $c\vec{E}_r \times \vec{B}/B^2$ ) drives a modified two-stream insta-

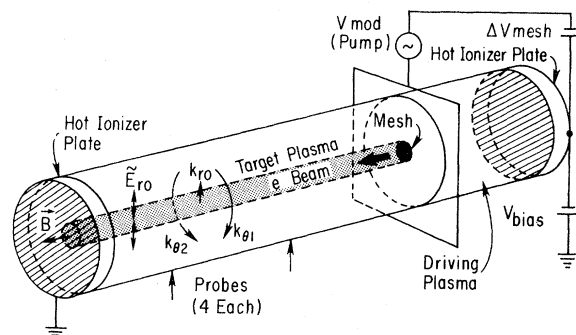


FIG. 1. Schematic of beam-plasma system.

bility with a peak amplitude at the lower-hybrid frequency and localized near the beam edge.<sup>5</sup> In the present experiment,  $V_{\text{bias}}$  is sufficiently small that this wave is not excited.

Superimposition of a modulated voltage ( $V_{\text{mod}} \sim 1$  V peak to peak) on the mesh bias at a frequency  $\omega_0 \gtrsim \omega_{\text{LH}} \simeq (\omega_{pi}^2 + \omega_{ci}^2)^{1/2}$  (where  $\omega_{pe}/\omega_{ce} \ll 1$  and  $\omega_{pi}/\omega_{ci} \sim 7$ ) causes the beam density, and therefore the radial electric field, to oscillate at  $\omega_0$ . This pump wave decays into a lower-hybrid wave ( $\omega_2 = \omega_0 - \omega_1$ ) and a low-frequency decay wave ( $\omega_1 \sim \omega_{ci}$ ) where the subscripts 0, 1, and 2 denote the pump and the low- and high-frequency decay waves. The amplitudes of both decay waves are peaked at nearly twice the beam radius. Parametric decay occurs in discrete intervals of  $\omega_0$ , typically  $1 < \omega_0/\omega_{\text{LH}} < 2$  (most unstable regime),  $4.5 < \omega_0/\omega_{\text{LH}} < 6.5$ , and others up to  $\omega_0/\omega_{\text{LH}} = 27$  (upper limit of wave generator). A typical frequency spectrum is shown in Fig. 2(a). The fre-

quency-matching rule ( $\omega_0 = \omega_1 + \omega_2$ ) is strictly satisfied for all  $\omega_0$ .

The perpendicular wave numbers ( $\vec{k}_{\perp} = \vec{k}_{\theta} + \vec{k}_r$ ) were determined by measuring the phase shift between the signals detected by two probes as one probe was moved radially ( $k_r$ ) or rotated azimuthally ( $k_{\theta}$ ) with respect to the other. Figure 2(b) demonstrates  $k_{\theta}$  matching:  $k_{\theta 1} = -k_{\theta 2}$ ,  $k_{\theta 0} = 0$ . The decay waves have standing-wave structures in the radial direction where  $|k_{r0}| < |k_{r1}| \simeq |k_{r2}| < |k_{\theta 2}|$ , confirming  $k_r$  matching. The pump and decay waves are mixtures of traveling and standing waves in the axial direction. From the phase shift between two probes separated axially by  $L/3$  and aligned with  $B$ , we find that  $k_{z(0,1,2)} = 2\pi/NL$  with  $N = 1, 2$ , or 4 for each wave. The standing-wave structures, determined from calibrated wave-amplitude measurements at three probe positions separated by  $L/3$ , indicate  $k_z$  matching where  $|k_{z1}| = |k_{z2}| = \pi/2L = |k_{z0}|/2$ .

By comparing the experimental and theoretical dispersion relations ( $\omega_2$  vs  $k_{\perp 2}$ ), the high-frequency decay wave has been identified as a lower-hybrid wave (LHW) as shown in Fig. 3. The theoretical results are obtained from a numerical solution of the warm, fully magnetized plasma dispersion relation in a slab geometry.<sup>12</sup>

As candidates for the low-frequency decay wave ( $\omega_1 \sim \omega_{ci}$ ) one can consider the first ion

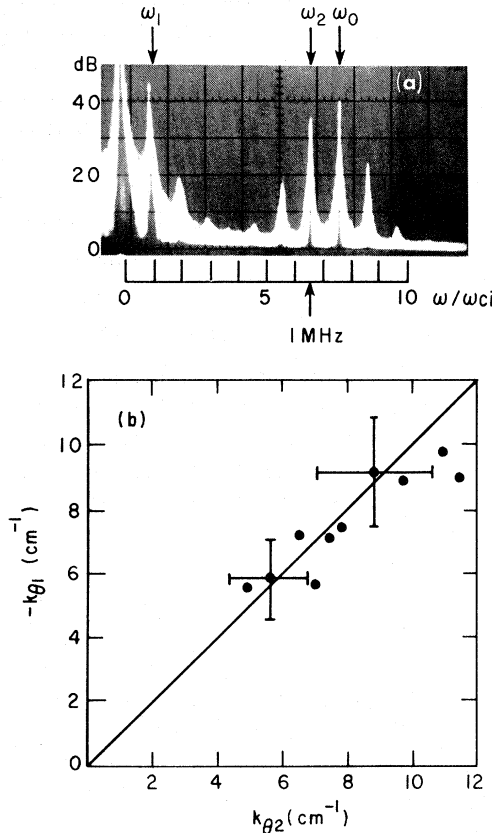


FIG. 2. (a) Typical frequency spectrum ( $\omega_{ci}/2\pi = 156$  kHz,  $\omega_{\text{LH}}/2\pi \simeq 1.1$  MHz). (b)  $k_{\theta}$  matching (solid line is  $k_{\theta 1} = -k_{\theta 2}$ ). Data points correspond to various  $\omega_0$  with all other parameters constant ( $1.40 \text{ MHz} \leq \omega_0/2\pi \leq 1.53$  MHz).

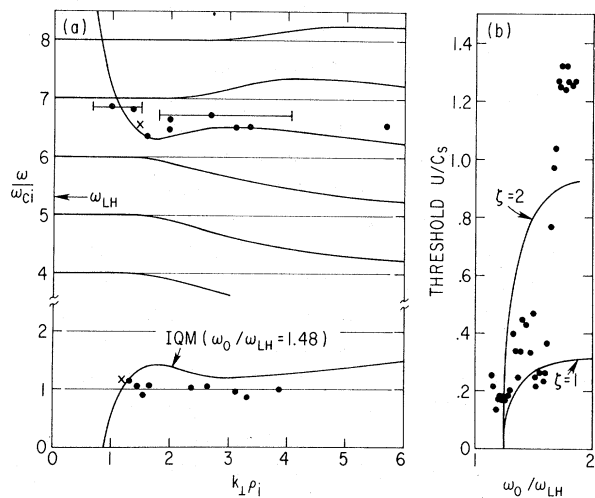


FIG. 3. (a) Dispersion relations of LHW and IQM. Unlabeled solid curves are the ion-Bernstein and LHW dispersion relation ( $\rho_i^2 = 2T_i/m_i\omega_{ci}^2$ ). The ten LHW (upper) and ten IQM (lower) data points result from ten different  $\omega_0$  ( $1.40 < \omega_0/\omega_{\text{LH}} < 1.53$ ); error bars indicate experimental uncertainty in  $k_{\perp 1,2}$ . (b) Threshold pump power vs  $\omega_0$ , data and theory (Ref. 7).

Bernstein mode (IBW,  $\omega_1/k_{z1}v_e \gg 1$ ,  $1.25 < \omega_1/\omega_{ci} < 2$ ), the ion-cyclotron wave (ICW,  $\omega_1/k_{z1}v_e \ll 1$ ,  $1 < \omega_1/\omega_{ci} < 1.15$ ), and the ion quasimode (IQM) which has maximum growth rate<sup>10</sup> for  $\omega_1/k_{z1}v_e \approx 1$ , where  $v_e^2 = 2T_e/m_e$ . Experimentally, we find that  $\frac{1}{3} < \omega_1/k_{z1}v_e < 3$  and  $0.4 < \omega_1/\omega_{ci} < 1.25$  for all  $\omega_0$ , and the IQM requirements are always satisfied. The ICW requirements are occasionally met for  $\omega_0 > 1.2\omega_{LH}$ , but the ICW dispersion relation is not satisfied. The IBW is not found.

In the theory of parametric decay into a LHW and an IQM, the LHW is a normal mode [ $\epsilon(\omega_2, k_2) = 0$ ] satisfying the dispersion relation as shown in Fig. 3(a). For a given  $\omega_0$ , the IQM is a forced oscillation with  $\omega_1$  and  $k_1$  determined by  $\omega_1 = \omega_0 - \omega_2$  and  $k_{\perp 1} = -k_{\perp 2}$  (since  $k_{\perp 0} \approx 0$ ). Thus, each different  $\omega_0$  results in a similar IQM curve, but shifted in frequency. A typical IQM curve for  $\omega_0/\omega_{LH} = 1.48$  is shown in Fig. 3(a). The IQM and LHW data points for  $\omega_0/\omega_{LH} = 1.48$ , indicated by  $\times$ 's, both lie close to their respective theoretical curves. IQM curves (not shown) for each of the other nine  $\omega_0$  values must show similar agreement with the IQM data points since  $\omega$  and  $k_{\perp}$  matching and the LHW dispersion relation are satisfied. A numerical solution of the IQM theory predicts maximum growth rates for  $k_{\perp \rho i 1} \sim 2$ , as observed.

Assuming an electrostatic pump wave of the form  $E = E_0 \cos(\omega_0 t - \vec{k}_0 \cdot \vec{x})$ , where  $k_{z0} \ll k_{\theta 0} < k_{r0}$  and  $k_{z0}k_{z1}/k_{r0}k_{\theta 1} < \omega_0/\omega_{ce} \ll 1$ , the dominant term in the parametric coupling coefficient is  $\mu = c\vec{E}_r \cdot \vec{k}_{\theta 1}/B\omega_0$ , corresponding to the axial drift of the electrons.<sup>7</sup> For  $\mu \ll 1$ ,  $|\chi_{i,e}(\omega_2)| \ll |\chi_{i,e}(\omega_1)|$ , and ignoring the decay wave at the upper sideband of the pump, the dispersion relation for the parametric decay of the pump wave is<sup>7,10</sup>

$$\epsilon(\omega)\epsilon(\omega_0 - \omega) + \frac{1}{4}\mu^2\chi_i(\omega)\chi_e(\omega) = 0, \quad (1)$$

where  $\epsilon(\omega)$  and  $\epsilon(\omega_0 - \omega)$  are the dielectric constants of the IQM and LHW, and  $\chi_{i,e}(\omega)$  are the ion and electron susceptibilities of the IQM.

In Fig. 3(b) the calculated threshold pump amplitude<sup>7</sup> is plotted versus  $\omega_0$  and compared with the measured threshold ( $U/C_s = c\vec{E}_{r0}/BC_s$ ) which is the lowest pump level, for a given  $\omega_0$ , at which decay waves are discernible above the plasma noise. Here  $C_s^2 = T_e/m_i$ , and  $\vec{E}_{r0} = k_{r0}\vec{\phi}_0$  is the fluctuating pump potential which is measured with a calibrated Langmuir probe.<sup>12</sup> The theoretical threshold is determined by the electron collisional damping of the LHW,  $\nu_e = 0.3\omega_{ci}$  in this experiment, and by electron Landau damp-

ing of the IQM (phase velocity,  $\zeta = \omega_1/k_{z1}v_e \approx 1-2$ ).<sup>7</sup> The agreement between experiment and theory is quite satisfactory considering that we have neglected the fine structure of  $\chi_i$ .<sup>10</sup>

An important consequence of this instability is the observed strong perpendicular ion heating and its possible implications for lower-hybrid or electron-beam heating in fusion plasmas.<sup>13</sup> To investigate the time dependence of the instability amplitude and the ion heating, the modulated mesh voltage (pump) was pulsed on (rise time  $< 1 \mu\text{sec}$ ) for 400  $\mu\text{sec}$ . As seen in Fig. 4(a) the amplitudes of both decay waves grow, saturate, and fluctuate together as expected. Parallel and perpendicular ion temperatures were measured using a small (2 mm diam) gridded Faraday cup positioned where the decay waves have maximum

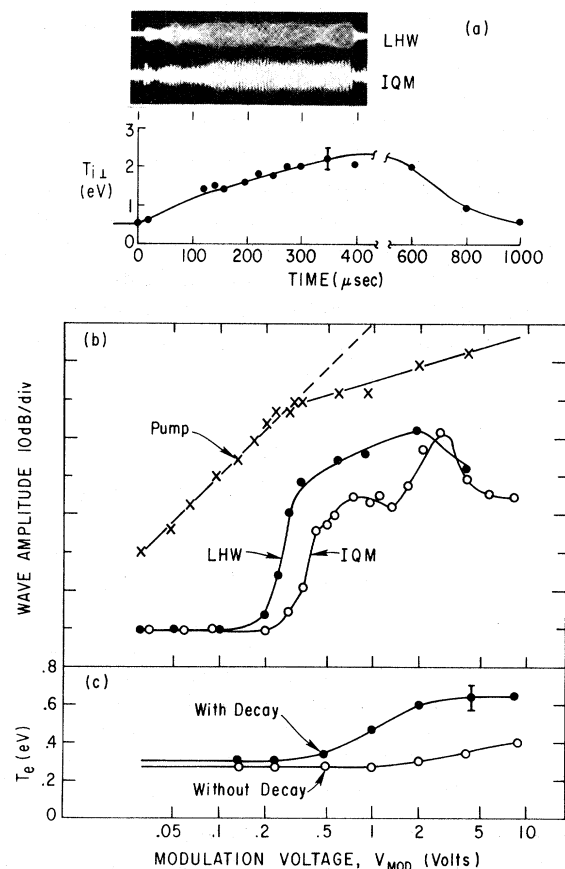


FIG. 4. (a) Decay-wave amplitudes and  $T_{i\perp}$  vs time.  $V_{\text{mod}}$  (pump) is applied for  $0 \leq t \leq 400 \mu\text{sec}$ . Decay-wave signals at  $t < 20 \mu\text{sec}$  are due to ringing from  $V_{\text{mod}}$  pulse. (b) Pump and decay-wave amplitudes vs  $V_{\text{mod}}$ . (c)  $T_e$  vs  $V_{\text{mod}}$ . Closed circles, with the parametric instability present; open circles, for a pump frequency without decay.

amplitude. The collector current signal is sampled with a resolution of 5  $\mu$ sec. In Fig. 4(a), one sees a pronounced increase of  $T_{i\perp}$  as the decay waves grow, without much change in  $T_{i\parallel}$ . Although this ion heating can be partly due to ion-cyclotron damping of the IQM, the perpendicular interaction of the LHW<sup>5</sup> with the ions is likely to cause most of the  $T_{i\perp}$  increase and the observed tail formation.

With the onset of the instability, one observes an enhanced absorption of the pump wave as shown in Fig. 4(b) where we have plotted the amplitudes of the pump, the LHW, and the IQM as functions of  $V_{m\text{od}}$ . The associated increase in  $T_e$ , plotted in Fig. 4(c), appears to be due to electron Landau damping of the IQM for which  $\zeta \approx 1$ . The increase in  $T_e$  is limited by the heat conduction loss to the end plate. Furthermore, for pump frequencies without parametric decay, the increases of  $T_i$  and  $T_e$  were small when compared with the heating when parametric instabilities were excited.

In summary, we have demonstrated that by modulating the density of an electron beam at or above  $\omega_{\text{LH}}$  the heating efficiency of both electrons and ions in a target plasma can be greatly increased. This increase is associated with the parametric excitation of lower-hybrid waves and ion-cyclotron quasimodes. Similar effects may be expected during heating of tokamaks with rf near  $\omega_{\text{LH}}$ . Furthermore, similar heating tech-

niques can be applied by modulating a beam at other plasma eigenmode frequencies.

This work was supported in part by Bell Laboratories and in part by the U. S. Department of Energy Contract No. EY-76-02-3073.

<sup>1</sup>J. D. Sethian *et al.*, Phys. Rev. Lett. **40**, 451 (1978); J. Chang *et al.*, Phys. Rev. Lett. **34**, 1266 (1975).

<sup>2</sup>K. Papadopoulos and K. Palmadesso, Phys. Fluids **19**, 605 (1976); I. Alexeff *et al.*, Phys. Rev. Lett. **25**, 848 (1970).

<sup>3</sup>G. M. Haas and R. A. Dandl, Phys. Fluids **10**, 678 (1967); V. P. Bhatnagar and W. D. Getty, Phys. Fluids **15**, 2222 (1972).

<sup>4</sup>K. Yatsui and T. Imai, Phys. Rev. Lett. **35**, 1279 (1975).

<sup>5</sup>M. Yamada and D. K. Owens, Phys. Rev. Lett. **38**, 1529 (1977).

<sup>6</sup>M. Porkolab, in *Proceedings of the Symposium on Plasma Heating in Toroidal Devices, Varenna, Italy, 1974* (Editrice Compositori, Bologna, 1974), p. 41.

<sup>7</sup>M. Porkolab, Phys. Fluids **17**, 1432 (1974).

<sup>8</sup>A. Rogister, Phys. Rev. Lett. **34**, 80 (1975).

<sup>9</sup>R. L. Berger and F. W. Perkins, Phys. Fluids **19**, 406 (1976).

<sup>10</sup>M. Porkolab, Phys. Fluids **20**, 2058 (1977).

<sup>11</sup>M. Ono *et al.*, Princeton Plasma Physics Laboratory Report No. PPPL-1395, 1977 (unpublished).

<sup>12</sup>S. Seiler and M. Yamada, Princeton Plasma Physics Laboratory Report No. PPPL-1412, 1978 (unpublished); S. Seiler, Ph.D. thesis, Princeton University, 1975 (unpublished).

<sup>13</sup>M. Porkolab *et al.*, Phys. Rev. Lett. **38**, 230 (1977).

## Diffuse-Boundary Rayleigh-Taylor Instability

Edward Ott and David A. Russell

*Department of Electrical Engineering, Cornell University, Ithaca; New York 14853*

(Received 24 July 1978)

For density profiles,  $N(y)$ , making a smooth transition from  $N(-\infty)=0$  to  $N(+\infty)=\text{const}$  with  $d \ln N/dy$  decreasing monotonically with  $y$ , it is shown that the Rayleigh-Taylor instability exhibits essentially different behavior above and below a certain critical wave number,  $k_c$ . For  $k > k_c$  the growth of the response to an initial perturbation is slower than exponential,  $\sim t^{-1/2} \exp(\gamma_b t)$ . For  $k < k_c$  an unstable eigenmode (analogous to that in the sharp boundary case) exists, and purely exponential growth occurs.

Recently, as a result of developments in pellet fusion,<sup>1</sup> imploding liner fusion,<sup>2</sup> and ionospheric physics,<sup>3,4</sup> the Rayleigh-Taylor instability has been the subject of renewed interest. In this note we present results for the Rayleigh-Taylor instability with a diffuse density profile. For a fairly broad class of profiles we find that there exists a critical wave number (transverse to the

density gradient) above which there are no eigenmode solutions, and the time-asymptotic response to an initial excitation exhibits slower than exponential growth. For smaller wave numbers eigenmode solutions occur, and the time-asymptotic response to an initial perturbation grows exponentially with time.

Taking gravity  $\vec{g} = -g\vec{Y}_0$  with equilibrium density

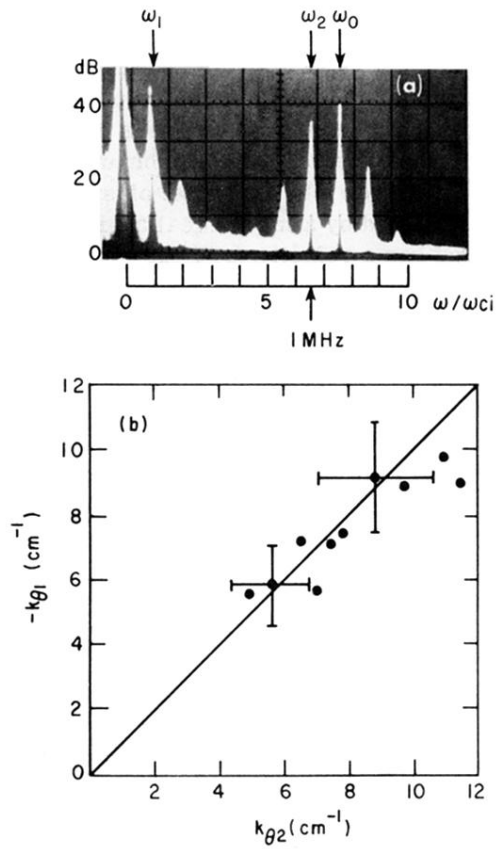


FIG. 2. (a) Typical frequency spectrum ( $\omega_{ci}/2\pi = 156$  kHz,  $\omega_{LH}/2\pi \approx 1.1$  MHz). (b)  $k_{\theta}$  matching (solid line is  $k_{\theta 1} = -k_{\theta 2}$ ). Data points correspond to various  $\omega_0$  with all other parameters constant ( $1.40 \text{ MHz} \leq \omega_0/2\pi \leq 1.53$  MHz).

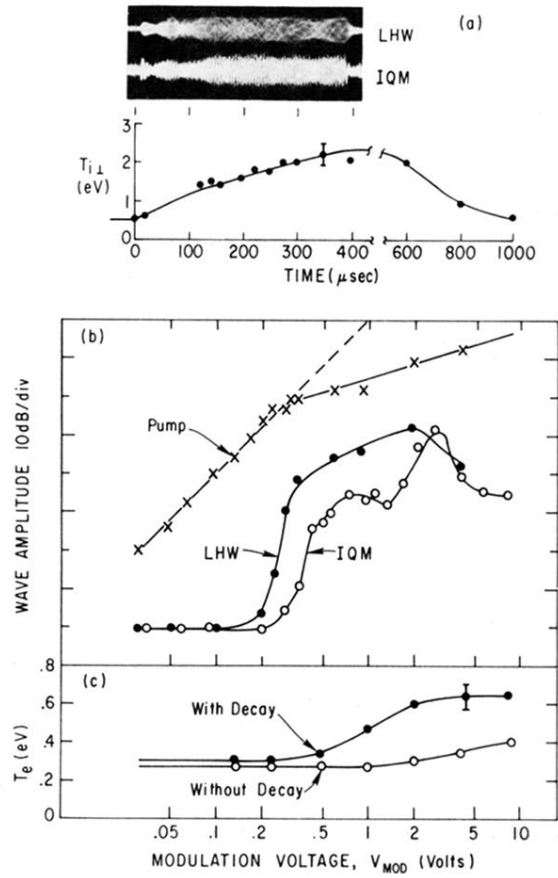


FIG. 4. (a) Decay-wave amplitudes and  $T_{i\perp}$  vs time.  $V_{\text{mod}}$  (pump) is applied for  $0 \leq t \leq 400 \mu\text{sec}$ . Decay-wave signals at  $t < 20 \mu\text{sec}$  are due to ringing from  $V_{\text{mod}}$  pulse. (b) Pump and decay-wave amplitudes vs  $V_{\text{mod}}$ . (c)  $T_e$  vs  $V_{\text{mod}}$ . Closed circles, with the parametric instability present; open circles, for a pump frequency without decay.